Multibody approach to model toothbrush bristles elasto-kinematics

Alessio Cellupica[1], **Luca D'Angelo**[2], **Marco Cirelli**[2], **Marta Mazur**[3], **Pier Paolo Valentini**[1]

[1] Department of enterprise engineering
University of Rome Tor Vergata
Via del Politecnico 1, 00133, Italy
alessio.cellupica@alumni.uniroma2.eu
valentini@ing.uniroma2.it

[2] Department of mechanical engineering
University Niccolò Cusano
Via Don Carlo Gnocchi 3, 00166, Italy
marco.cirelli@unicusano.it
luca.dangelo@unicusano.it

[3] Department of dental and maxilo-facial sciences
University of Rome La Sapienza
Sapienza Piazzale Aldo Moro 5 00185, Rome, Italy
Marta.mazur@uniroma1.it

ABSTRACT

Brushing is a specific procedure that aims to remove biofilms from vertical and occlusal tooth surfaces and as much as possible from interdental spaces. The most common question about toothbrush development is the estimation of contact force for the assessment of cleaning performance and safety. It depends on the bristles that represent the contact elements of the toothbrush. The deformation of the bristles cannot be studied using linear models or two-dimensional approaches because they have a large deflection. Nonlinear beam models are computationally demanding since exact closed-form expressions are not available for large complex deformations. Multibody methodology represents a very suitable approach to analyze this problem because it is possible to provide information about contact forces and sliding forces, bristles deformation, and can be a valid tool for improving the design of bristles. In this paper, two multibody models, able to consider large deflection, have been adopted. The first is a simplified model based on the Larry Howell PRB 2D model, which splits the beam into two segments connected by a spherical joint and a lumped bushing element. The second is the discrete flexible approach, based on more detailed rigid body discretization and elastic lumped elements. Both methods are compared with quantitative experimental results that reproduce the toothbrush's cleaning on the reference surfaces.

Keywords: Flexible Multibody System, Contact, Pseudo-rigid body model.

1 INTRODUCTION

One of the dentistry topics represents identifying the forces necessary for the efficient removal of plaque on the teeth without causing damage to the soft tissues. The development of toothbrushes no longer based on the use of tufts, but with bristles has led the scientific community to deepen the study of the interaction forces between toothbrush and tooth. In particular, the study focused on the evaluation of the forces exerted by the bristles in contact with a surface. Brushing has been extensively studied in the field of periodontology and dental hygiene since the 1960s [1]. The effectiveness of brushing is based on empirical data obtained from clinical investigations, standardization of patients and practices, and periodic testing of toothbrushes [2, 3]. There is a direct correlation between the force used and the effectiveness of brushing up to a certain threshold value, above which there is no longer a direct correlation [4]. Mathematical models and in vitro investigations have been used to characterize brushing. The best bristles were created

using mathematical data to provide maximal therapeutic effectiveness and little harm to soft and hard tissue [5, 6, 7]. Various mathematical models have been used to study brushing performance, evaluating bristle modulus, diameter, length, cross-sectional shape, and composition to explain toothbrush stiffness [8, 9, 10]. Analytical methods, finite element analysis, and flexible multibody techniques have all been used to study bristle models for brushing on flat or curved surfaces [11, 12, 13]. The pseudo-rigid body approach was used to represent the compliance of the brush, and a comparison of analytical and experimental results has been done [14, 15]. These studies have provided insights into the motion of bristles, contact between the brush and oral biofilm, enamel, and soft tissue, and the efficacy of different brush configurations for specific applications such as road sweeping and satellite detumbling [16, 17]. During tooth brushing, the bristles are subjected to a very large three-dimensional deflection, impacts, jamming, buckling, and other nonlinear phenomena due to the highly complex tooth geometry with asperities, tight gaps, and peaks. Due to the amount, typology, and nonlinear contact mechanics [25, 26], the bristle's deformation cannot be studied using linear models or two-dimensional approaches. It requires complex numerical models to be simulated since exact closed-form expressions are not available for large complex deformations [18]. Therefore, a trustworthy and more inclusive numerical technique is required for computing quantitative performance indices and contrasting various design solutions or operational situations. This paper aims to compare different pseudo-rigid models, based on multibody equations [19], that is Howell 2D PRB model [20, 21] and Discrete Flexible Multibody ones (DFM) [22, 23, 24], about the interaction between the bristles of a brush and a planar surface in terms of tangential and normal contact forces. These approaches are used to model a toothbrush in silicone (E = 7.5 Mpa); an experimental model is assembled to have the bristle deformation feedback and to compare the contact forces with Multibody models. The paper is organized as follows: in the first part, the multibody models are explained, and the application of these approaches to the toothbrush is illustrated in Figure 1. Then the experimental assembly is described, with significant accuracy in data acquisition. In the last part, the results of the bristles deformation and the contact forces from multibody models are presented, then compared with real model assembly results.

Figure 1: *Toothbrush adopted for the study.*

2 MULTIBODY MODELS AND METHODOLOGIES

The first step of this paper consists of the explanation of the Multibody models used to evaluate the deformation and the contact forces of the bristles. The first method is an extension of the Howell pseudo-rigid body approach to a 3D case [20, 21, 25]. This approache splits the beam into two segments connected by a spherical joint and a lumped bushing element. The second one is discrete flexible multibody (DFM) [22, 23, 24], based on more detailed rigid body discretization and elastic lumped elements [26, 27]. Then follow the application of the models on the toothbrush for different cases of study.

2.1 Howell 2D pseudo-rigid body model

In 2D case, the bristle could be considered like a flexible cantilever beam with constant cross-section and linear material properties; the case is of a beam non-follower end loaded. If the

deflections are large, they may be out of the range of linearised beam deflection equations; however, the flexible beam's pseudo-rigid body model offers a straightforward yet accurate way to analyze the deflection of flexible beams. For a flexible cantilever beam with a force at the free end, large-deflection elliptic-integral equations demonstrate that the free end follows a nearly circular path. Based on this consideration, Howell develops a pseudo-rigid model where, the nearly circular path, can be accurately modeled by two rigid links joined at a pivot along the beam. A torsional spring at the pivot represents the beam's resistance to deflection. The location of this pseudo-rigid body characteristic pivot is measured from the beam's end as a fraction of the beam's length, where the fractional distance is γl and γ is the characteristic radius factor. The coefficient γ is deduced from the ratio:

$$n = \frac{F_n}{F_t} \tag{1}$$

Where the term n is the reciprocal of the friction coefficient μ for the specific contact configuration:

$$n = \frac{1}{\mu} \tag{2}$$

If the friction coefficient is known, it could be used the Tab.1 to compute γ and, consequently the coefficient K_Θ, which is the characteristic stiffness parameter of the PRB model.

Table 1: *Numerical data for n, γ, K_Θ*

n	γ	K_Θ
0.0	0.8517	2.67617
0.5	0.8430	2.63744
1.0	0.8360	2.61259
1.5	0.8311	2.59289
2.0	0.8276	2.59707
3.0	0.8232	2.56737
4.0	0.8207	2.56506
5.0	0.8192	2.56251
7.5	0.8168	2.55984
10.0	0.8156	2.56597

From these coefficients, it could determine the torsional spring stiffness k and the revolute joint position:

$$k_{Tor} = \gamma K_\Theta \frac{EI}{l} \tag{3}$$

Where E is the Young modulus of the bristle, I is the Inertia modulus of the cross-section of the bristle with respect to the direction of the inflection plane, l is the bristle length.

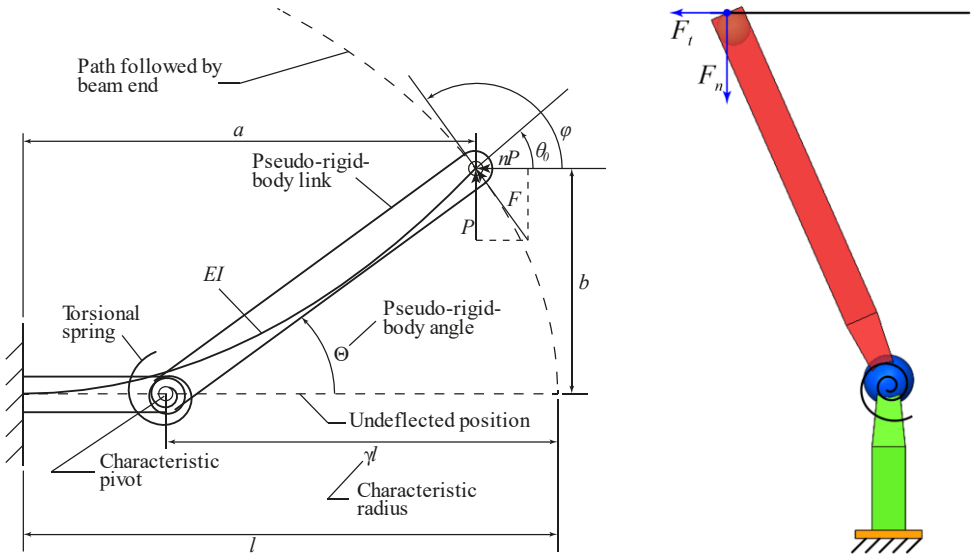

Figure 2: *a) Cantilevered beam with forces at the free end and its pseudo-rigid-body model. b) Application of Howell PRB model to the toothbrush.*

For the specified case the Howell 2D PRB model is extended to 3D case in both deflection plans. However, this approach lacks accuracy because it supposes that the mixed contributions of inflection are null, so the path followed from the beam end is a sphere. Generally, the path drawn from the beam end is an elliptic surface [25]. For the torque contribution, the respective stiffness is calculated from the cross-section of the pseudo-rigid body link. Figure 2a shows the Howell 2D PRB model scheme, while Figure 2b shows the application of the model to the toothbrush. The friction coefficient used is $\mu = 0.76$, which is the friction coefficient for the contact between a silicone toothbrush and a plexiglass surface. From Tab. 1, with linear interpolation, $\gamma = 0.8329$ and $K_\Theta = 2.6001$. The bristles of the toothbrush shown in Figure 1 have different lengths, so it needs some iteration to determine the spring stiffness and the revolute joint bristle for each beam; some bristles don't touch the surface, so the Multibody model creates the PRB model only if the bristle length is major than the distance between the brush base and the plexiglass surface.

2.2 Discrete Flexible Multibody model (DFM)

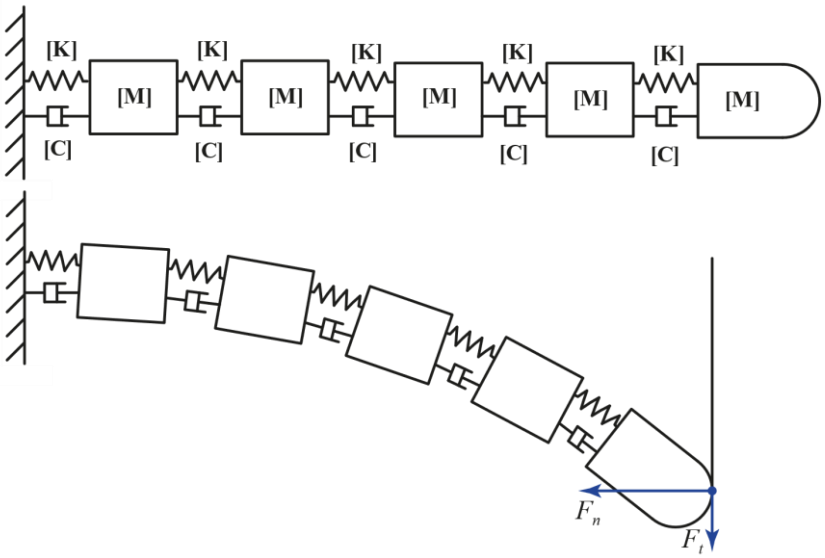

Figure 3: *The discrete rigid body model of a bristle.*

Although the DFM's basic concept is similar to the PRB model, it may describe structural deflection and contact mechanics in greater detail due to the DFM's implementation. The bristle is divided into multiple nodes in the DFM (Figure 3), each of which has six degrees of freedom and its mass and inertia (called rigid body nodes). Due to stiffness matrices, which produce

reaction forces and moments based on the relative displacement between coordinate reference systems of adjacent nodes, adjacent nodes interact with one another. In other words, it is possible to think of the stiffness matrices as a set of springs attached to each pair of neighboring nodes and triggered whenever a relative displacement occurs. The Timoshenko beam theory can be used to determine the general stiffness matrix acting between two nodes [23]:

$$[\boldsymbol{K}]_{i,i+1} = \begin{bmatrix} \frac{EA}{L} & 0 & 0 & 0 & 0 & 0 \\ 0 & \frac{12EI_{zz}}{L^3(1+P_y)} & 0 & 0 & 0 & \frac{-6EI_{xx}}{L^2(1+P_y)} \\ 0 & 0 & \frac{12EI_{yy}}{L^3(1+P_z)} & 0 & \frac{6EI_{yy}}{L^2(1+P_z)} & 0 \\ 0 & 0 & 0 & \frac{GI_{xx}}{L} & 0 & 0 \\ 0 & 0 & \frac{6EI_{yy}}{L^2(1+P_z)} & 0 & \frac{(4+P_z)EI_{yy}}{L(1+P_z)} & 0 \\ 0 & \frac{-6EI_{xx}}{L^2(1+P_y)} & 0 & 0 & 0 & \frac{(4+P_y)EI_{zz}}{L(1+P_y)} \end{bmatrix} \tag{4}$$

where

$$P_y = \frac{12EI_{zz}A_{sy}}{GAL^2} \tag{5}$$

$$P_z = \frac{12EI_{yy}A_{sz}}{GAL^2} \tag{6}$$

A_s is the shear area ratio, E is the Young's Modulus, G is the shear modulus, A is the section area, L is the distance between adjacent nodes and I_{jj} is the moment of inertia of the cross-section concerning j-axis. As a result, the forces and moments between the adjacent nodes can be expressed as:

$$\vec{F}_{i,i+1} = [\boldsymbol{K}]_{i,i+1} \cdot \vec{\Delta}_{i,i+1} \tag{7}$$

where $\Delta_{i+1,i}$ is the vector of relative displacements (translational and rotational) between the nodes' generalized coordinates.

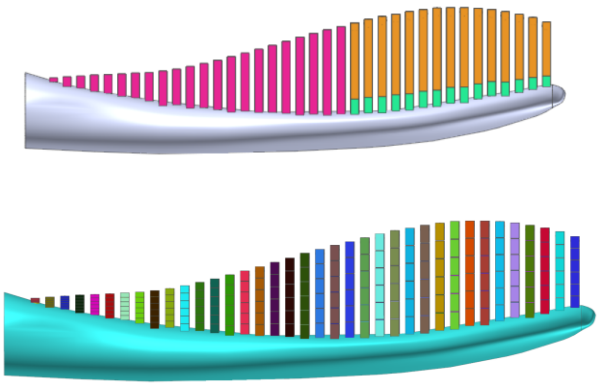

Figure 4: Application of a) Howell PRB model and b) DFM model to the toothbrush.

The DFM is applied on the toothbrush bristles as shown in Figure 4, the grade of the discretization is enough to evaluate the bending and torsional contributions of stiffness. Each bristle end with a sphere, like in Howell PRB model, to reduce the computational burden due to contact interaction.

2.3 Contact mechanism

Figure 2b shows that each pseudo-rigid body link ends with a sphere. Introducing these dummies bodies simplifies the contact computation from body-body to sphere-surface contact and reduces consequentlu the computational burden. Because there are a lot of surfaces in contact (between the bristles and the plexiglass plane), so the sphere-surface contact [28] is faster to resolve than solid-solid contact and could reduce the computational burden [29]. For the purpose of finding contact points, an effective search method is required. The algorithm is defined on a pre-searching for contact zones and a detailed-searching for contact region penetration depth. The contact force generated at the contact point is based on a penalty contact force (8), from the Hertz theory [28, 30], and developed by Flores [31]. The base surface is approximated with a multi-triangular mesh, while the action surface is discretized with n contact points. The contact formulation [32, 33] allows calculating the normal force through the relation:

$$F_n = k\delta^{m_1} + c\frac{\dot{\delta}}{\left|\dot{\delta}\right|}\left|\dot{\delta}\right|^{m_2}\delta^{m_3} \tag{8}$$

where:

- $\delta, \dot{\delta}$ are the penetration and its speed;
- m_1, m_2 and m_3 are the exponents of stiffness, damping, and indentation factor, respectively;
- k and c are the stiffness and damping coefficients.

The tangential contact force is then computed using Equations (1),(2) and applied along the direction opposite to the sliding velocity at the contact point:

$$F_t = -\mu F_n \frac{v_t}{\|v_t\|} \tag{9}$$

where $\boldsymbol{v}_t$ is the sliding velocity at the contact point (perpendicular to the normal vector). The contact between the bristles is neglected to reduce the computational burden. However, this contribution is important for a generalization of the problem, because when the direction of motion changes, the interaction between the bristles leads to a reduction of normal forces as they come into contact with each other, exerting less pressure on the flat surface.

3 EXPERIMENTAL SETUP

The experimental setup was designed to have feedback on the deformation of the bristles. A photometric comparison between the experiment and the models is performed to verify the reliability of the models. The toothbrush has been constrained on a support able to slide on a flat transparent surface adopting an armonic motion. To visualize the bristles' physical deformation, a fixed camera is installed on the frame. The experimental bench was built using a stepper motor, a TB6600 Stepper Motor Driver which consists of a driver that can control a two-phase bipolar stepper motor, two Arduino Mega 2560 boards, an analog joystick, a lead screw linear actuator and a 12V transformer. The Arduino Mega 2560 boards have the function, respectively, of managing the movement of the two-phase bipolar stepper motor, controlled by an analog joystick, and of acquiring the load cell data in parallel with the movement. The acquisition of the signals obtained from the load cells takes place via buttons that activate the recording of the values of interest. The movement of the toothbrush is managed by a stepper motor, connected to the lead screw linear actuator. On the slider are located 2 load cells, respectively one measures the normal contact load and the other one the tangential contact load. Two supports were created using 3D printing, the first one connects the load cells, and the second one is screwed to the topper load cell and is the housing of the toothbrush. Figure 5b shows the connection system of the toothbrush, load cells and slider, while Figure 5a shows the experimental bench.

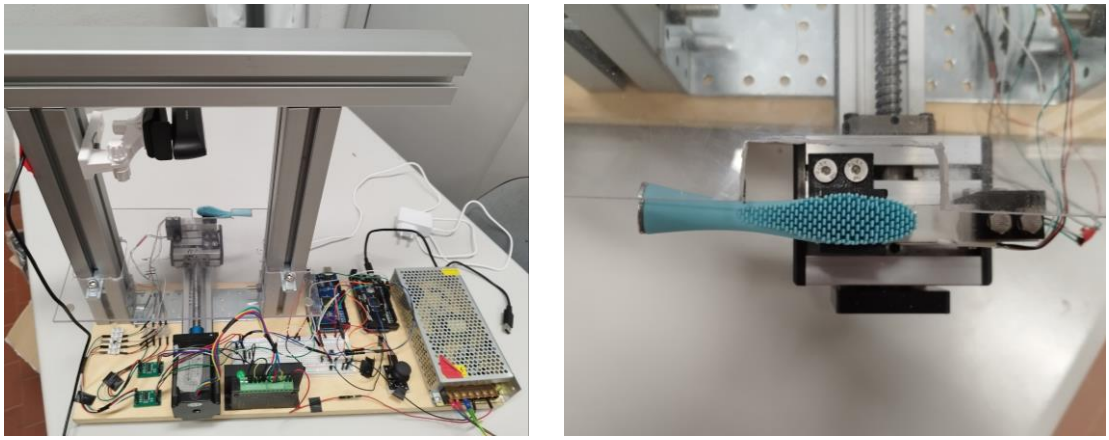

Figure 5: *a) Complete experimental bench b) Toothbrush grabbing and movement setup.*

4 RESULTS AND DISCUSSIONS

The following paragraph shows the results obtained from the Multibody simulations. Fig. 6 shows the deformations of the bristles to have a visual comparison of the results obtained. The Fig. 6a, 6d, 6g, 6l, 6o, 6r show the toothbrush direction motion from top to bottom, the bristles deflection follows the brush motion. The Fig. 6b, 6e, 6h, 6m, 6p, 6s show the buckling bristles configuration when the directrion motion changes, so when the brushing motion is stopped. The Fig. 6c, 6f, 6i, 6n, 6q, 6t show the toothbrush return from bottom to top. As can be seen, the Discrete Flexible Multibody model is likely to represent the deformations of the physical bristles (it should be emphasized that the absence of contact between the bristles leads to a slight discrepancy in the physical results). The Howell model, on the contrary, does not follow the physical model in terms of bristle deformation for obvious reasons: in deformation terms, the pseudo-rigidbody link of the Howell model does not have the deformation degrees of freedom by definition of the Multibody model. The Howell PRB model can not represent and solve the real buckling phenomena, because the discretization is based on two rigid bodies instead of multiple ones. Therefore, a perturbation force is needed to face the directional change. However, the goal of brushing is the force applied by the user on the teeth, rather than the deformation of the bristles, so more attention has been paid to evaluating these forces.

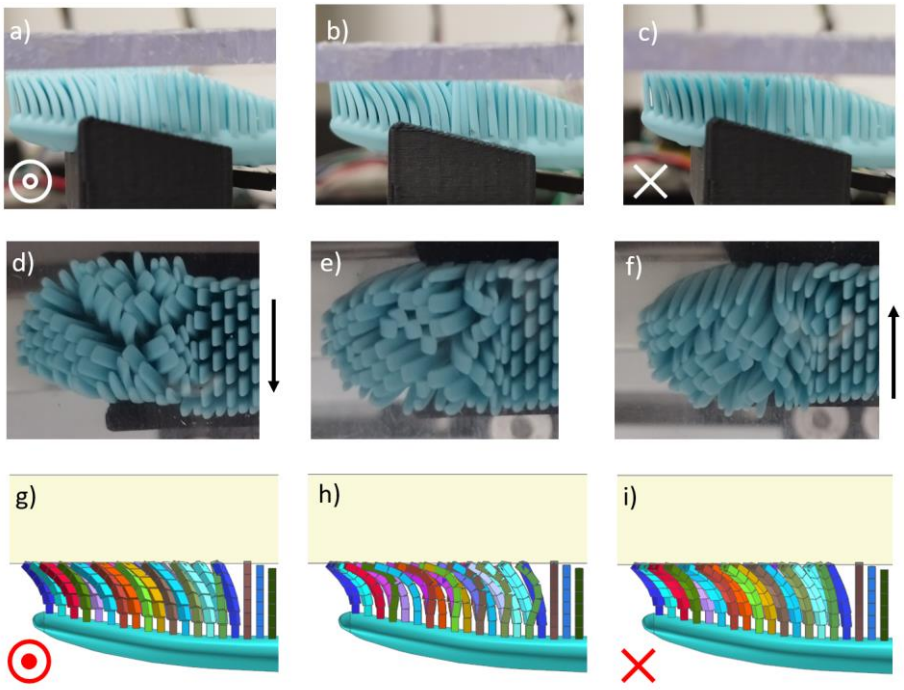

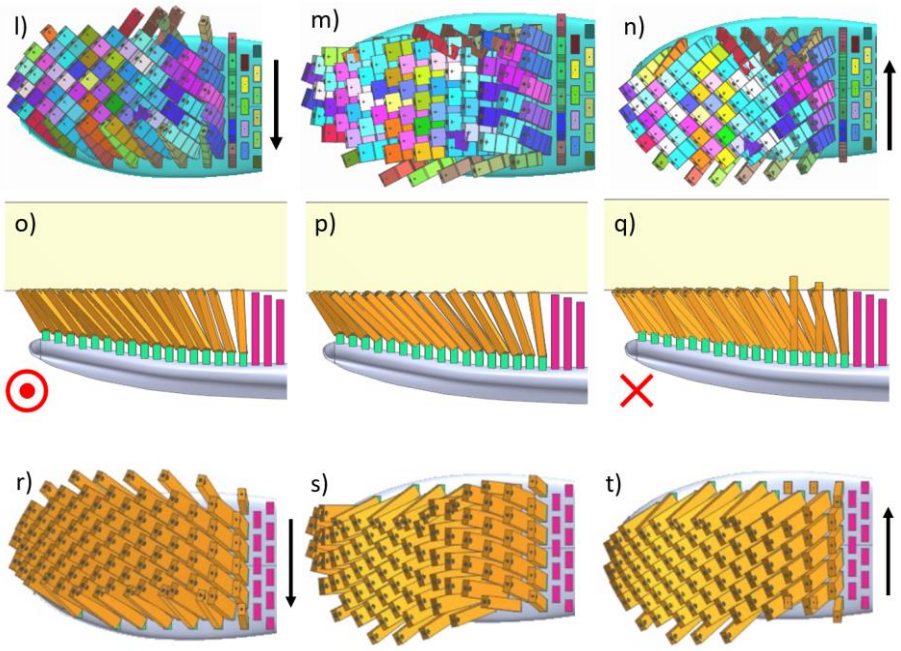

Figure 6: *Visualization of the frames for the 2 pseudo-rigid models and the physics model.*

Figure 7 compares the results obtained from the pseudo-rigid models and the real model in terms of normal force,, tangential force and friction coefficient. The initial peaks are due to the condition of incipient buckling which occurs in the first reversal of the direction of motion. The results of the Howell model show another peak at the second change in direction of motion, resulting from the inability of the model to resolve the buckling of some bristles. Peak force occurs when the maximum penetration limit is reached for some bristles. It can be seen in Figure 6q that for 4 bristles the unstable condition causes excessive penetration, resulting in loss of contact. The presence of perturbation forces allows the solver to resolve the indentation condition. In subsequent reversals of motion, the peak forces remain larger for the Howell model than for the experimental case and the DFM model due to the greater stiffness of the rigidbody link: the normal force peaks are twice the DFM ones and four times the experimental ones. In the brushing phase, the normal forces in the experimental case show asymmetry as a function of the direction of motion. This asymmetry is related to the mutual interaction between the bristles and the compliance of the supports in the experimental model. The error in normal force during brushing between the experimental and Howell models has a maximum of about 18% and a minimum of about 5%; between the experimental and DFM, the error is in the range of 16% and 1.6%. The Howell model, which requires less computational time than the DFM, yields results for the normal force that closely match the experimental model. Nevertheless, to overcome the loss of contact near the change in direction of motion, it would be appropriate to use a model that is a trade-off between the Howell discretization and the DFM one. Tangent forces are related to normal forces according to relation (9), so the discussion will be about the coefficient of friction. It is important to note that during the reversal phase of motion prior to brushing (approximately constant force), all models exhibit a sinusoidal trend in tangential forces. In particular, the excessive stiffness exhibited by Howell's model is reflected in a change in the direction of the tangential forces. The dynamic friction coefficient is close to 0.76 for the multibody models; for the experimental model, this coefficient varies as a function of both the actual roughness of the flat surface, but also because of the yielding of the supports of the surface inflection itself. In fact, a maximum increase of about 13% in the friction coefficient can be seen compared to the nominal working conditions.

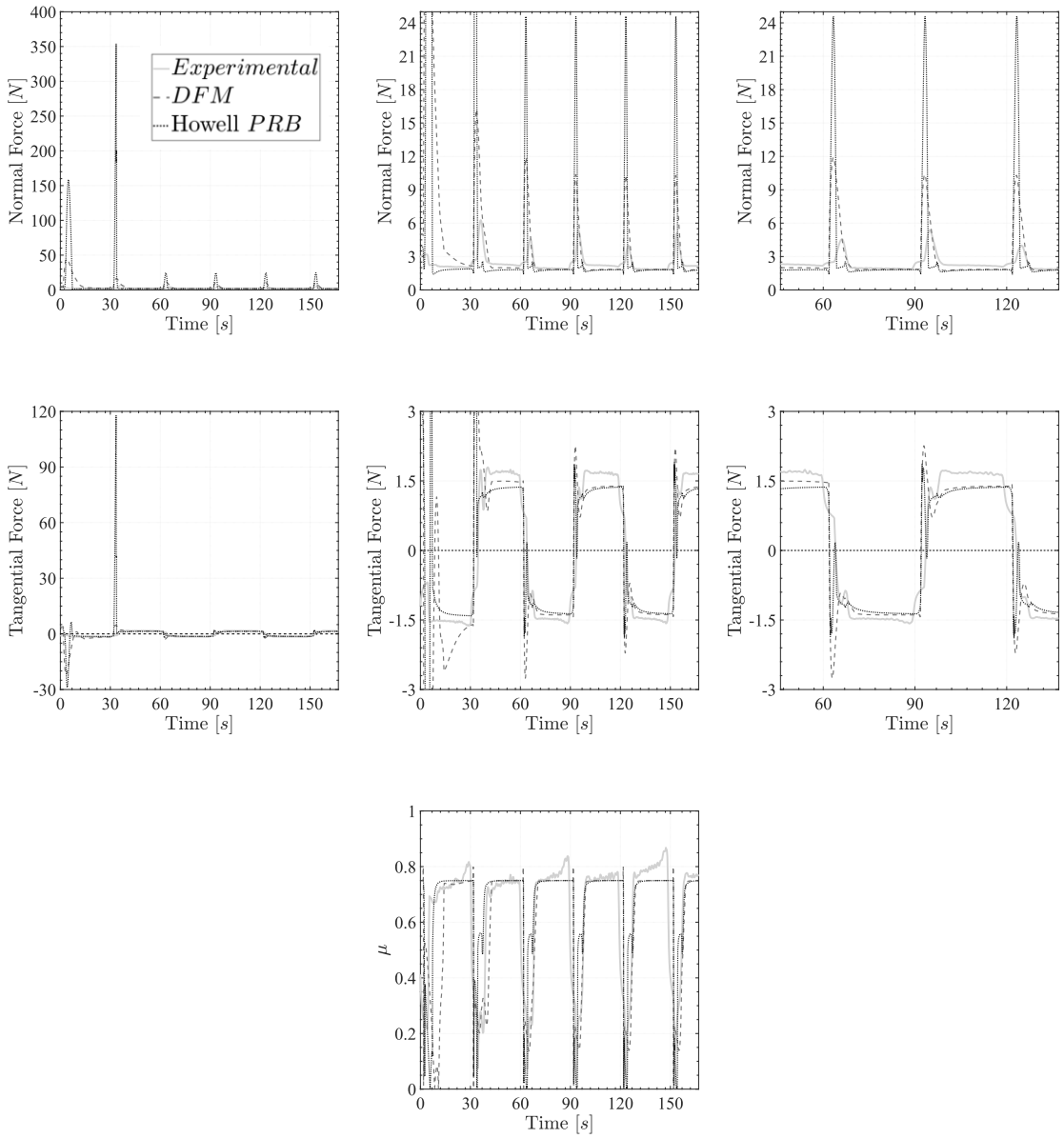

Figure 7: *Comparison of the results obtained for the normal force (top), tangential force (middle), coefficient of friction (bottom).*

5 CONCLUSIONS

In conclusion, in this paper, two multibody models have been developed and compared, such as the Howell PRB model and the Discreet Flexible Multibody model, to evaluate the contact forces that the bristles of a toothbrush exert on a flat surface. The solutions are compared with the experimental setup to analyse the correctness of the large deflection of the bristles through visual feedback and to compare the contact forces. From the results, it was obtained that both multibody models return contact force values that mirror those obtained from the experimental model. The Howell model has fewer onerous calculation times, however, the excessive stiffness causes instability on the contact, due to an excessive penetration, near the variation of the direction of motion. Therefore, it is necessary to implement an external perturbation. Furthermore, for obvious reasons, the deformation does not reflect that of the experimental model. Therefore, DFM shows advantages both in terms of contact force and in terms of deformation.Nevertheless, for greater accuracy of the results, it would be useful to introduce the contact between the different bristles and consider the deformation and interaction phenomena linked to this contribution.

References

[1] I. Bay, K. M. Kardel and M. R. Skougaard, "Quantitative evaluation of the plaque-removing ability of different types of toothbrushes," The Journal of Periodontology, vol. 38, pp. 526-533, 1967.

[2] J. A. Gibson and A. B. Wade, "Plaque removal by the Bass and Roll brushing techniques.," Journal of periodontology, vol. 48, pp. 456-459, 1977.

[3] H. B. G. Robinson, "Toothbrushing habits of 405 persons," The Journal of the American Dental Association, vol. 33, pp. 1112-1117, 1946.

[4] G. A. Van der Weijden, M. F. Timmerman, M. M. Danser and U. Van der Velden, "Relationship between the plaque removal efficacy of a manual toothbrush and brushing force," Journal of clinical periodontology, vol. 25, pp. 413-416, 1998.

[5] G. A. Van der Weijden, "Timmerman ME Nijboer A, Lie MA, van der Veiden U. A comparative study of electric toothbrushes for the ef-fectiveness of plaque removal in relation to toothbrushing dura-tion—Time study," J Clin Periodontol, vol. 20, pp. 476-481, 1993.

[6] H. R. Rawls, N. J. Mkwayi-Tulloch and M. E. Krull, "A mathematical model for predicting toothbrush stiffness," Dental Materials, vol. 6, pp. 111-117, 1990.

[7] E. Kaiser, M. Meyners, D. Markgraf, U. Stoerkel, R. Koppenfels, R. Adam, M. Soukup, H. Wehrbein, C. Erbe and others, "Brush head composition, wear profile, and cleaning efficacy: an assessment of three electric brush heads using in vitro methods," J Clin Dent, vol. 25, pp. 19-25, 2014.

[8] G. P. J. Langa, F. W. M. G. Muniz, T. P. Wagner, C. F. Silva and C. K. Rösing, "Anti-plaque and anti-gingivitis efficacy of different bristle stiffness and end-shape toothbrushes on interproximal surfaces: a systematic review with meta-analysis," Journal of Evidence Based Dental Practice, vol. 21, p. 101548, 2021.

[9] J. R. Heath and H. J. Wilson, "Classification of toothbrush stiffness by a dynamic method.," British Dental Journal, vol. 130, pp. 59-66, 1971.

[10] I. S. Organization, "Dentistry-Stiffness of the Tufted Area of Toothbrushes," Standards Document ISO 8627, 1987.

[11] R. J. Stango, V. Cariapa, A. Prasad and S.-K. Liang, "Measurement and analysis of brushing tool performance characteristics, part 1: stiffness response," 1991.

[12] V. Cariapa, R. J. Stango, S.-K. Liang and A. Prasad, "Measurement and Analysis of Brushing Tool Performance Characteristics, Part 2: Contact Zone Geometry," 1991.

[13] S. M. Heinrich, R. J. Stango and C. Y. Shia, "Effect of workpart curvature on the stiffness properties of circular filamentary brushes," 1991.

[14] C.-Y. Shia, R. J. Stango and S. M. Heinrich, "Analysis of contact mechanics for a circular filamentary brush/workpart system," 1998.

[15] E. Uhlmann and C. Sommerfeld, "Dynamic contact analysis of abrasive filaments with a discrete system," in Proceedings of the 20th International Symposium on Advances in Abrasive Technology, 2017.

[16] E. Uhlmann and C. Sommerfeld, "Three-dimensional dynamic contact analysis of abrasive filaments with a multi-body system," Procedia CIRP, vol. 72, pp. 615-621, 2018.

[17] Z. Ma, Z. Liu, H. Zou and J. Liu, "Dynamic modeling and analysis of satellite detumbling using a brush type contactor based on flexible multibody dynamics," Mechanism and Machine Theory, vol. 170, p. 104675, 2022.

[18] P. P. Valentini and E. Pennestrì, "Modeling elastic beams using dynamic splines," Multibody system dynamics, vol. 25, pp. 271-284, 2011.

[19] F. Cheli, E. Pennestrì and others, Cinematica e dinamica dei sistemi multibody, volume 2, CEA Casa Editrice Ambrosiana, 2009.

[20] L. L. Howell, "Compliant mechanisms," in 21st Century Kinematics: The 2012 NSF Workshop, 2013.

[21] Y.-Q. Yu, L. L. Howell, C. Lusk, Y. Yue and M.-G. He, "Dynamic modeling of compliant mechanisms based on the pseudo-rigid-body model," 2005.

[22] R. L. Huston and Y. Wang, "Flexibility effects in multibody systems," Computer-Aided Analysis of Rigid and Flexible Mechanical Systems, pp. 351-376, 1994.

[23] J. R. Hutchinson, "Shear coefficients for Timoshenko beam theory," J. Appl. Mech., vol. 68, pp. 87-92, 2001.

[24] O. A. Bauchau and S. Han, "Advanced Beam Theory for Multibody Dynamics," in International Design Engineering Technical Conferences and Computers and Information in Engineering Conference, 2013.

[25] N. O. Rasmussen, J. W. Wittwer, R. H. Todd, L. L. Howell and S. P. Magleby, "A 3d pseudo-rigid-body model for large spatial deflections of rectangular cantilever beams," in International Design Engineering Technical Conferences and Computers and Information in Engineering Conference, 2006.

[26] M. Cera, M. Cirelli, L. Colaiacovo and P. P. Valentini, "Second-order approximation pseudo-rigid model of circular arc flexure hinge," Mechanism and Machine Theory, vol. 175, p. 104963, 2022.

[27] P. P. Valentini and E. Pennestrì, "Elasto-kinematic comparison of flexure hinges undergoing large displacement," Mechanism and Machine Theory, vol. 110, pp. 50-60, 2017.

[28] W. C. Young, R. G. Budynas and A. M. Sadegh, Roark's formulas for stress and strain, McGraw-Hill Education, 2012.

[29] M. Autiero, M. Cera, M. Cirelli, E. Pennestrì and P. P. Valentini, "Review with Analytical-Numerical Comparison of Contact Force Models for Slotted Joints in Machines," Machines, vol. 10, p. 966, 2022.

[30] V. L. Popov and others, Contact mechanics and friction, Springer, 2010.

[31] P. Flores, M. Machado, M. T. Silva and J. M. Martins, "On the continuous contact force models for soft materials in multibody dynamics," Multibody system dynamics, vol. 25, pp. 357-375, 2011.

[32] J. Choi, H. S. Ryu, C. W. Kim and J. H. Choi, "An efficient and robust contact algorithm for a compliant contact force model between bodies of complex geometry," Multibody System Dynamics, vol. 23, pp. 99-120, 2010.

[33] J. Choi, S. Rhim and J. H. Choi, "A general purpose contact algorithm using a compliance contact force model for rigid and flexible bodies of complex geometry," International Journal of Non-Linear Mechanics, vol. 53, pp. 13-23, 2013.